Tunnelling characterization of quantum interference effects in confined geometries

1993 J. Phys.: Condens. Matter 5 1975

(http://iopscience.iop.org/0953-8984/5/13/013)

J. Phys.: Condens. Matter 5 (1993) 1975–1982. Printed in the UK

Tunnelling characterization of quantum interference effects in confined geometries

Y Takagaki and D K Ferry

Center for Solid State Electronics Research, Arizona State University, Tempe, AZ 85287-6206, USA

Received 5 October 1992, in final form 25 January 1993

Abstract. We have performed quantum-mechanical calculations of tunnelling current drained through a narrow probe weakly attached to quantum wires. The amplitude of the current is approximately proportional to the local density of states in the wires. We demonstrate that the spatial variation of the probability distribution of an electron due to quantum interference effects is obtained by scanning the probe along the wires.

1. Introduction

In microstructures with dimensions less than the phase coherence length—the distance over which the electron phase information is retained—the transport properties are dominated by quantum interference effects. If the microstructure is in the dirty metal limit, an electron incident on the device is scattered from impurities and defects. The interference caused by scattering from different impurities leads to phenomenon such as the $h/2e$ magnetoresistance oscillation in a ring geometry [1], weak localization [2], and universal conductance fluctuations (UCF) [3]. In clean materials, for which the elastic mean free path can be larger than the sample size, scattering from the sample boundaries plays an alternative role. Resonant conduction through zero-dimensional states has been observed in experiments [4]. Under these circumstances, the multiple reflections of the electron wave within the device results in a spatial variation of the local density of states [5, 6].

A recent experiment by Eugster and del Alamo [7] demonstrated that the density of states in one-dimensional structures can be measured by means of tunnelling spectroscopy. Suppose that an additional narrow probe is weakly coupled to the devices. A tunnelling current leaking out through a barrier potential is roughly proportional to the density of states and provides tunnelling spectroscopy through sweeping the Fermi energy at low temperatures, where the density of states varies slowly on the scale of k_BT [7, 8]. If the width of the tunnelling probe is reduced to be comparable to the Fermi wavelength, the tunnelling current will measure a local density of states modified by the quantum interference effects.

In this paper, we propose an experiment in which the tunnelling current is measured while the tunnelling probe is scanned along the quantum wires. The amplitude of the current as a function of the coordinates provides a mapping of the probability distribution of an electron in the device, a concept well known in the field of scanning tunnelling microscopy (STM).

0953-8984/93/131975+08$07.50

2. Numerical model

The model structures are illustrated in figure 1. They have a T-shaped geometry. The lead is attached at a right angle to the horizontal wire and is used to detect the tunnelling current leaking out a thin side wall of the wire. We confine our analysis to a two-dimensional plane of infinitesimal thickness. This plane is patterned to form the quantum wire structures. We consider two types of device in which to investigate the effects of quantum interference on the tunnelling current: (*a*) a narrow-wide-narrow (NWN) junction and (*b*) a wire with two impurities. In the former device the width of the wire is widened to D over a length L. The wide region acts as a resonator, analogous to electromagnetic waveguides, and the forward transmission probability shows narrow dips due to resonance as D is varied [9]. In the latter device, multiple reflections between the two impurities cause constructive and destructive interferences in the transmission probability as the separation between impurities is varied [10, 11].

Suppose that an electron with energy $E_F = \hbar^2 k_F^2/2m$ is incident through the left-hand semi-infinite lead. In the absence of the side lead, the electron is either reflected with probability T_B or transmitted with probability T_F. We introduce an additional lead attached to the main channel through a barrier potential represented as a shaded area in figure 1. We assume a thin ($d/W = 0.1$) uniform potential barrier with height $U = 50E_F$. An electron is transmitted into the side lead with probability T_S. To evaluate the transmission coefficients, we use a waveguide-matching technique [12, 13]. The quantum wires are divided into a sequence of uniform waveguide sections, in which the wave function can be composed of a linear combination of standing wave solutions. The wave function is then matched across the interfaces between adjacent sections. We assume a hard-wall confinement potential in the transverse direction of the wire. We have checked that a sufficient number of modes are included in the calculation so that including more modes has little influence on the results. We restrict, for simplicity, our discussion to the case where electrons are incident only through the lowest mode in the semi-infinite lead. When more than two modes are occupied at the Fermi energy, the total current is given as a superposition of contributions from each incident mode.

3. Results and discussion

3.1. Characterization of zero-dimensional states

Let us first discuss the results on the NWN geometry. The forward transmission probability T_F is plotted in figure 2(*a*) as a function of $k_F W/\pi$ in the absence of the side probe. The dimensions of the wide region are $D/W = 1.3$ and $L/W = 3.1$. A system similar to our ($L \sim W$) has been discussed in detail by Sols *et al* [14]. The increase in the width lowers the threshold energy of the transverse mode and quasibound states split off from one of the evanescent modes. The transmission probability shows narrow dips when the Fermi energy coincides with the quasibound state levels. We label the dips with nearly perfect reflection A, B, C and D as indicated in figure 2(*a*). In figures 2(*b*) and 2(*c*), we show the tunnelling probability T_S for two values of the position of the side lead a/W. Since the coupling of the side lead to the main channel is weak, T_F is not altered significantly. Therefore, we do not show T_F in the presence of side lead. In general, the energy dependence of T_S reveals narrow peaks coinciding with the dips in T_F [8]. Note that the electron

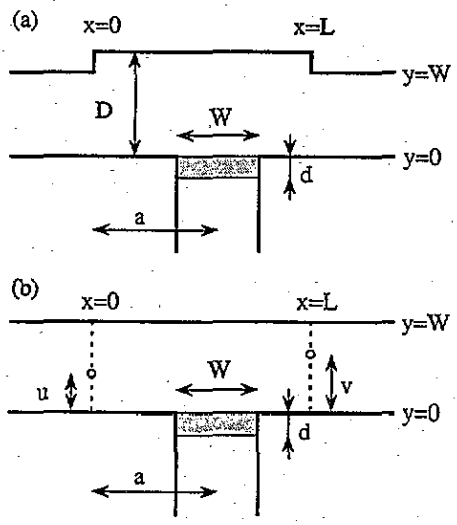

Figure 1. Configuration of the system. A side lead is attached to the main channel through a tunnelling barrier, represented by the shaded area, in which a barrier with height U is assumed. (*a*) The resonant structures occur in the transmission probabilities due to the presence of quasi-bound states in the wide-region. (*b*) The open circles indicate two δ-function impurities in a quantum wire.

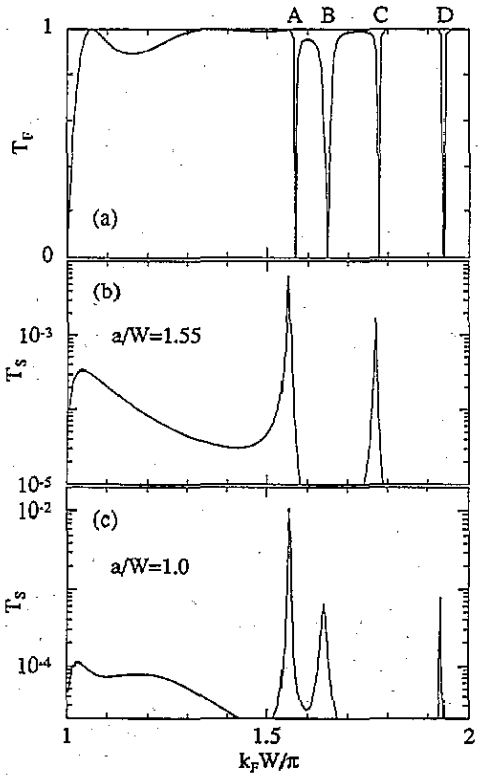

Figure 2. Transmission probabilities as a function of $k_F W/\pi$ in the narrow-wide-narrow structure with $D/W = 1.3$ and $L/W = 3.1$. (*a*) Forward transmission probability T_F in the absence of the side lead. The dips of nearly perfect reflection are labelled A–D. Transmission probability T_S into the side lead is plotted for (*b*) $a/W = 1.55$ and (*c*) $a/W = 1.0$.

confinement in the wide region is weakened by the presence of the side lead, and hence the resonance energies are lowered. This is the reason that the dips in T_F (calculated in the absence of the side lead) and the peaks in T_S appear at slightly different energies in figure 2.

The tunnelling probability is related to the density of states $g_j(E_F - E_j)$ in the probed region. At $T = 0$ we have [7]

$$T_S = \frac{2\pi\hbar^2}{m} \sum_j k_{\perp j} T_j(E_F - U) g_j(E_F - E_j) \tag{1}$$

where the sum is over occupied one-dimensional subbands in the wire. The normal wave number $k_\perp$ incident on the tunnelling barrier is independent of energy. Therefore, the tunnelling current gives a direct view of the density of states by sweeping Fermi energy provided that the energy dependence of the transmission coefficient T_j at the Fermi energy across the barrier is negligible. It has been shown

that the increase of width creates narrow peaks in the density of states related to the quasibound states [6]. One notices that no peaks corresponding to the dips B and D are observed when the side probe is placed at the centre of the wide region and the peak corresponding to dip C disappears when $a/W = 1.0$. This gives us an idea of tunnelling microscopy of electron states by scanning the tunnelling probe along the wire.

The resonance conditions in the NWN geometry are described by

$$k_F^2 = (n\pi/D)^2 + (m\pi/L_{eff})^2 \tag{2}$$

where $L_{eff} \geqslant L$ represents the effective length of the wide region due to the open boundary at the exits to the narrow wires, and $L_{eff} \to L$ in the limit $D \gg W$. The probability distribution of the electron wave function at the resonances is displayed in figure 3. We find that the dips A, B, C and D correspond, respectively, to (n, m) = (2,1), (2,2), (2,3) and (2,4) with L_{eff} = 3.2~3.4. The structures in T_F and T_S at $k_F W/\pi < 1.5$ may be ascribed to the resonances with $n = 1$. In figure 4, we show three-dimensional plots of the tunnelling probability as functions of the normalized Fermi wave number and the coordinate along the wire. As a/W is varied for fixed $k_F W/\pi$, T_S shows a multiple peak structure and the number of peaks is increased for the higher energy resonances in accordance with the standing wave pattern shown in figure 3. One can see that the tunnelling probability is enhanced when the side lead is placed near the maximum of the probability distribution, reflecting the large local density of states. Note that for dip A the resonance energy is lowered by a large amount compared to the resonance width when the side lead is placed near the centre of the wide region. The tunnelling probability, therefore, shows a double-peak structure if the energy is fixed at the higher-energy tail of the resonance.

3.2. Characterization of quantum states scattered from impurities

Let us discuss another case where quantum interference plays an essential role in determining the conductance of the system. Coherent scattering from multiple impurities in confined geometry causes an oscillatory behaviour of the probability distribution of an electron. This strongly affects the conductance of the wire as a function of Fermi energy. The conductance modification is observed at low temperatures as aperiodic fluctuations when the Fermi energy or an external magnetic field is varied. To illustrate the tunnelling characterization of UCF we consider the simplest case shown in figure 1(*b*), where a δ-function potential is assigned for each impurity:

$$U_{imp}(x, y) = V_1\delta(x)\delta(y - u) + V_2\delta(x - L)\delta(y - v). \tag{3}$$

Since we are dealing with confined geometries, the δ-function potential causes mode mixing [15]. The two δ-function impurities are located in the wire (u/W = 0.34 and v/W = 0.57) with a separation of several times the wavelength (L/W = 3.1). We assume equal strength of the repulsive impurity potential to be $mV_i/\hbar^2 = 5$ with m the effective mass of an electron.

The forward transmission probability in a device without a side lead is shown in figure 5(*a*). The oscillation occurs due to multiple reflections between impurities. The characteristics of this resonance are that the peaks become broader in energy and the transmission at the minima becomes larger for larger $k_F W/\pi$. The energies

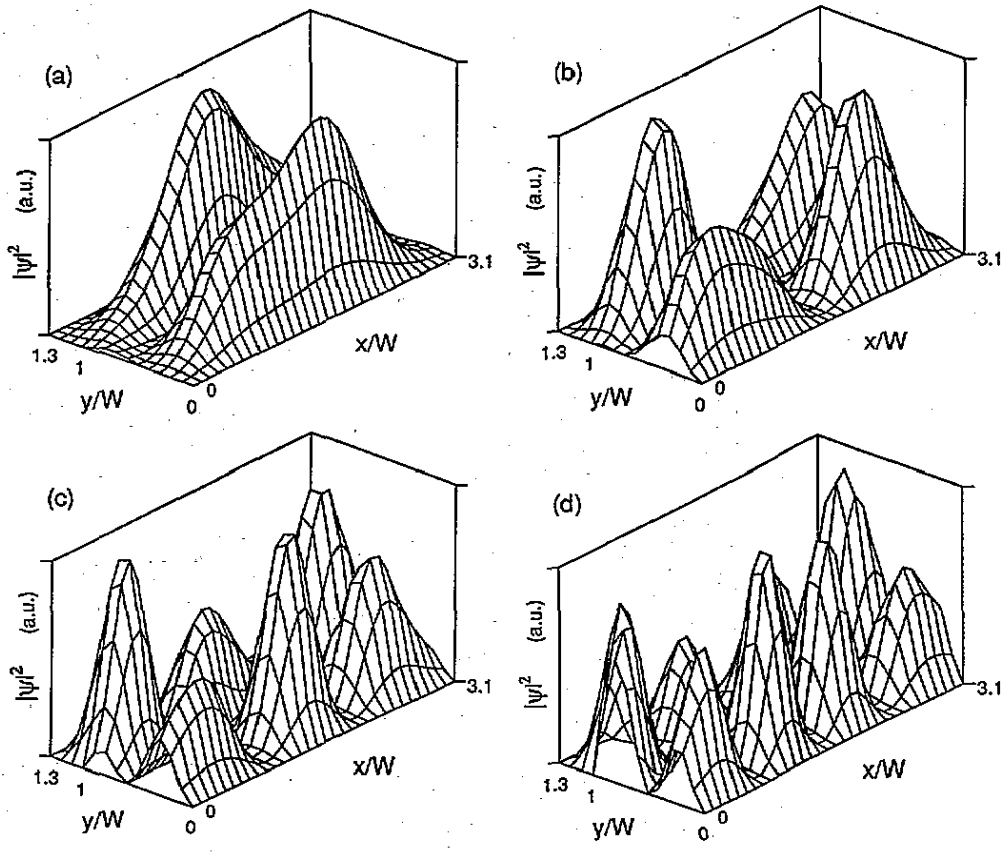

Figure 3. Probability distribution in the wide region at the resonances labelled (*a*) A, (*b*) B, (*c*) C and (*d*) D.

at which the maxima occur are roughly given by the condition $i(\lambda_1/2) = L$ with λ_1 the longitudinal wavelength of the lowest mode in the wire [11]. One can see this in the probability distribution shown in figure 6. Since only the lowest transverse mode is occupied in the wire, we plot the magnitude of the wave function along the centre of the wire, i.e. $y/W = 0.5$. The tunnelling probability is increased when T_F is maximum as shown in figures 5(*b*) and 5(*c*). The peak near $k_F W/\pi = 2$ is due to a quasi-bound state originating from the second-lowest subband. Figure 5(*b*) again indicates that the even-parity resonances do not give rise to peaks in T_S if the side lead is placed in the middle between two impurities. One also finds in figure 5(*c*) that the peak in T_S due to the $i = 3$ resonance disappears for $a/W = 1.0$. Three-dimensional representation of the tunnelling probability shown in figure 7 indicates that the probability distribution can be obtained through the tunnelling current measurement. In contrast to the case of the NWN geometry, the resonances are broad in energy and the peak-to-valley ratio of T_S is not large, and hence the mapping of the probability distribution is obtained over the entire range of energy.

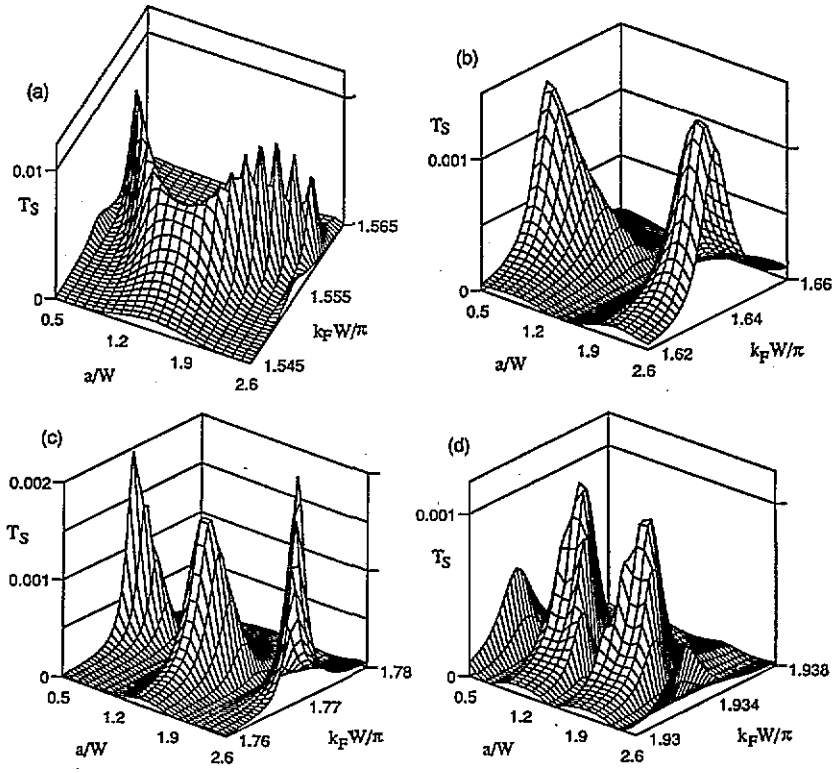

Figure 4. Tunnelling probability T_S as a function of the position of the side lead a/W and of the normalized Fermi wave number $k_F W/\pi$ for $W/D = 1.3$ and $L/W = 3.1$. The results (*a*)–(*d*) correspond to the dips A–D, respectively.

4. Concluding remarks

We have presented a numerical simulation of the tunnelling characterization of quantum waveguide structures. The results indicate that the spatial variation of the probability distribution due to quantum interference effects in the plane of the side lead can be obtained by means of tunnelling spectroscopy. An experiment may be performed by employing the STM technique with a fixed separation between the tip and the sample. The STM tip is located over the metal narrow wires and is scanned in the plane parallel to the sample. Our results suggest that the STM technique is useful in the study of mesoscopic systems. Impurity scattering is expected to be the dominant source of interference effects in metals. In this system, however, multi-subband effects will need to be taken into account because of the short wavelength of electrons. Microstructures created in GaAs–AlGaAs heterostructures, on the other hand, can provide clean single-mode devices, where the transmission resonances through the zero-dimensional states can be relatively easily observed. Unfortunately, the presence of surface depletion makes it difficult to measure the tunnelling current. Semiconductor materials free from surface depletion, such as InAs, will be appropriate materials for an experiment.

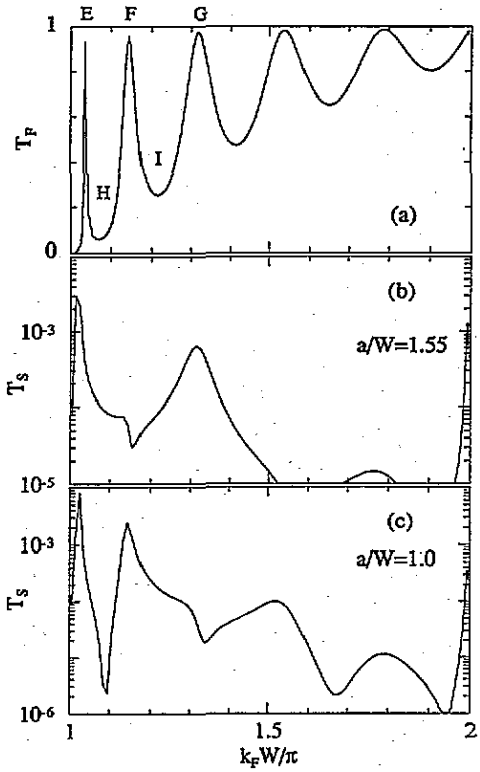

Figure 5. Transmission probabilities as a function of $k_F W/\pi$ in the double-impurity structure with $L/W = 3.1$. (*a*) Forward transmission probability T_F in the absence of the side lead. Several maxima and minima are labelled E–I. Transmission probability T_S into the side lead is plotted for (*b*) $a/W = 1.55$ and (*c*) $a/W = 1.0$.

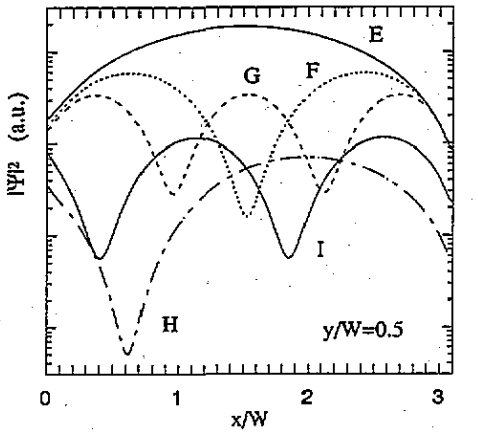

Figure 6. Probability distribution in the wire at the energies indicated as E–I in figure 5(*a*) for $y/W = 0.5$. Two impurities are placed at $x = 0$ and $x = 3.1$.

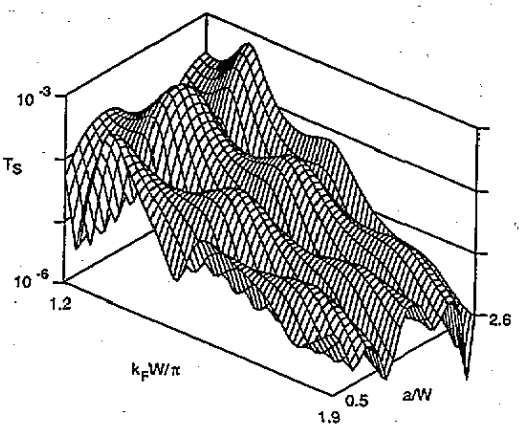

Figure 7. Tunnelling probability T_S in the double-impurity structure as a function of the position of the side lead a/W and of the normalized Fermi wave number $k_F W/\pi$.

Acknowledgment

This work was supported in part by the Office of Naval Research.

References

[1] Altshuler B L, Aronov A G and Spivak B Z 1981 *JETP Lett.* **33** 94
[2] Bergmann G 1984 *Phys. Rep.* **107** 1
[3] Lee P A and Stone A D 1985 *Phys. Rev. Lett.* **55** 1622
[4] Smith C G, Pepper M, Ahmed H, Frost J E F, Hasko D G, Peacock D C, Ritchie D A and Jones G A C 1988 *J. Phys. C: Solid State Phys.* **21** L893
[5] Thouless D J 1977 *Phys. Rev. Lett.* **39** 1167
[6] Itoh T, Sano N and Yoshii A 1992 *Phys. Rev.* B **45** 14131
[7] Eugster C C and del Alamo J A 1991 *Phys. Rev. Lett.* **67** 3586
[8] Takagaki Y and Ferry D K 1992 *Phys. Rev.* B **45** 12152
Takagaki Y and Ferry D K 1992 *J. Appl. Phys.* **72** 5001
[9] Sol F, Macucci M, Ravaioli U and Hess K 1989 *Appl. Phys. Lett.* **54** 350
[10] Kriman A M, Joshi R P, Haukness B S and Ferry D K 1989 *Solid State Electron.* **32** 1597
[11] Kumar A and Bagwell P F 1990 *Solid State Commun.* **75** 949
[12] Takagaki Y and Ferry D K 1991 *Phys. Rev.* B **44** 8399
[13] Cahay M, McLennan M and Datta S 1988 *Phys. Rev.* B **37** 10125
[14] Sol F, Macucci M, Ravaioli U and Hess K 1989 *J. Appl. Phys.* **66** 3892
[15] While δ-function potential causes no scattering in free space, this is not the case in confined systems. See [10] above as well as
Kriman A M and Ruden P P 1985 *Phys. Rev.* B **32** 8013
Kriman A M, Haukness B S and Ferry D K 1991 *Granular Nanoelectronics* ed D K Ferry, J R Barker and C Jacoboni (New York: Plenum) p 523